Topographic barriers drive the pronounced genetic subdivision of a range-limited fossorial rodent

Victoria M. Reuber[a], Michael V. Westbury[b], Alba Rey-Iglesia[b], Addisu Asefa[a], Nina Farwig[a], Georg Miehe[c], Lars Opgenoorth[d,e], Radim Sumbera[f], Luise Wraase[g], Tilaye Wube[h], Eline D. Lorenzen[b*] and Dana G. Schabo[a*]

[a] Department of Biology, Conservation Ecology, University of Marburg, Germany

[b] Globe institute, University of Copenhagen, Denmark

[c] Department of Geography, Vegetation Geography, University of Marburg, Germany

[d] Department of Biology, Plant Ecology & Geobotany, University of Marburg, Germany

[e] Swiss Federal Research Institute WSL, Birmensdorf, Switzerland

[f] Department of Zoology, University of South Bohemia, České Budějovice, Czech Republic

[g] Department of Geography, Environmental Informatics, University of Marburg, Germany

[h] Department of Zoological Sciences, College of Natural and Computational Sciences, Addis Ababa University, Ethiopia

* These authors contributed equally to this study

Correspondence: reuber@staff.uni-marburg.de

Keywords: mitogenomes, nuclear genomes, population structure, landscape genetics, conservation genetics

Abstract

Due to their limited dispersal ability, fossorial species with predominantly belowground activity usually show increased levels of population subdivision across relatively small spatial scales. This may be exacerbated in harsh mountain ecosystems, where landscape geomorphology limits species' dispersal ability and leads to small effective population sizes, making species susceptible to environmental change. The giant root-rat (*Tachyoryctes macrocephalus*) is a highly fossorial rodent confined to the afro-alpine ecosystem of the Bale Mountains in Ethiopia. Using mitochondrial and low-coverage nuclear genomes, we investigated 77 giant root-rat individuals sampled from nine localities across its whole ~1,000 km^2 range. Our data revealed a distinct division into northern and southern subpopulations, with no signs of gene flow, and higher nuclear genetic diversity in the south. Landscape genetic analyses of the mitochondrial genomes indicated that population subdivision was driven by steep slopes and elevation differences of up to 500 m across escarpments separating the north and south, potentially reinforced by glaciation of the south during the Late Pleistocene (~42,000 to 16,000 years ago). Despite the pronounced subdivision observed at the range-wide scale, weak geographic structuring of sampling localities within subpopulations indicated gene flow across distances of at least 16 km, suggesting aboveground dispersal and high mobility for relatively long distances. Our study highlights how topographic barriers can lead to the genetic subdivision of fossorial species, despite their potential to maintain gene flow at the local scale. These factors can reduce genetic variability, which should be considered when developing conservation strategies.

1. Introduction

The genetic subdivision and diversity of a species across space are determined by the combined effects of the environment and the ability of a species to disperse (Berthier et al., 2005; Manel et al., 2012; Quaglietta et al., 2013; Ruiz-Gonzalez et al., 2015). Dispersal ability can be limited by topographic barriers such as mountains or steep slopes, and by species-specific abiotic or biotic requirements, such as temperature or food availability, which may prevent the continuous distribution of individuals and reduce gene flow (Boulangeat et al., 2012; Cunningham et al., 2016; Cushman & Lewis, 2010; Sexton et al., 2009). As a consequence, natural selection, genetic drift, and inbreeding in smaller isolated populations may lead to heterogeneous patterns of genetic variability and population subdivision (Wright, 1969). Species with low dispersal ability such as those with low mobility and a burrowing lifestyle, are especially prone to these processes.

Fossorial rodents engineer elaborate underground burrow systems. In many species, activities including searching for mates, reproduction, and foraging, occur below-ground (Nevo, 1999). Therefore, these rodents are often restricted to specific soil types and available food resources (Begall et al., 2007; Nevo, 1999; Reichman, 1975). Apart from these notable constraints in habitat and resource availability, the low mobility of fossorial species leads to small home ranges and limited dispersal (Harestad & Bunnel, 1979; Tucker et al., 2014). As a result, fossorial rodents often have a localised and patchy distribution. Moreover, in the case of solitary species, mature individuals meet mainly during the mating season, which further limits conspecific encounters. Combined, these characteristics lead to small and isolated subpopulations, with low genetic variation and genetic differentiation across relatively small scales and rapid inter-population divergence, as shown for instance in several tuco-tuco species (*Ctenomys sp.,*) and common voles *(Microtus arvalis)* (Mapelli et al., 2012; Mirol et al., 2010; Nevo, 1999; Schweizer et al., 2007).

These genetic and ecological patterns may be exacerbated in harsh environments, such as in mountain ecosystems, where the geomorphology of the landscape and the availability of suitable

habitats, limits dispersal opportunities and leads to restricted species distribution ranges and small effective population sizes (Badgley et al., 2017; Brown, 2001; Gaston, 2003; Rahbek, Borregaard, Colwell, et al., 2019). As a result, mountain regions have been recognized as hotspots for genetic differentiation and speciation, contributing disproportionately to terrestrial biodiversity, at least in the tropics (Rahbek, Borregaard, Antonelli, et al., 2019; Rahbek, Borregaard, Colwell, et al., 2019; Sandel et al., 2011). However, species with limited distribution ranges and small population size, such as those found in mountain ecosystems, are at particular risk of extinction (Davies et al., 2009; Gaston, 2003). Small populations tend to exhibit accumulations of deleterious mutations, low intraspecific diversity, or loss of adaptive potential, making them susceptible to environmental change and habitat shifts (Hoffmann et al., 2017; Lande, 1988; Willi et al., 2006). Additionally, upslope habitat shifts are limited for mountain species, especially for those occurring near mountaintops (Parmesan, 2006; Wilson & Gutiérres, 2016). Mountain ecosystems face increasing threats from land use and climate change-induced habitat shifts. Therefore, it is imperative to understand the impact of species-environment interactions on genetic diversity to effectively establish conservation targets, however, thorough understanding is still lacking. Studying species in mountain ecosystems remains a challenge, especially for fossorial rodents, due to the difficulty of accessing remote areas and the inherent challenges in assessing these species in their natural habitats.

Our study addresses this knowledge gap by elucidating how landscape features drive the genetic subdivision and diversity of the giant root-rat (*Tachyoryctes macrocephalus*), a fossorial rodent endemic to the afro-alpine and afro-montane ecosystem of the Bale Mountains in southeast Ethiopia (Figure 1). The species has a limited distribution range of ~1,000 km^2 across the Bale Mountains massif and is found between 3,000 and 4,150 m above sea level (a.s.l.) (Sillero-Zubiri et al., 1995; Yalden & Largen, 1992). Giant root-rats have specific habitat requirements, occurring in grasslands in areas with good soil depth, especially along wetland shores and flooded valleys (Sillero-Zubiri et al., 1995; Šklíba et al., 2017). Grassland in river valleys that spread through shrubs and forest zones into lower

elevations, allow the species to expand down to about 3,000 m a.s.l. (Yalden, 1985). Their relatively small home ranges (about 100 m^2) can shift throughout the year depending on food availability (Šklíba et al., 2020). Giant root-rats are significant ecosystem engineers creating large underground burrow systems, in which they live solitarily. Through their combined effect of soil perturbation and herbivory, they alter nutrient availability, soil texture and moisture, and create their own habitat and that for other plant and animal species (Asefa et al., 2022; Miehe & Miehe, 1994; Šklíba et al., 2017; Yalden, 1985). By using below-ground burrows, the species circumvents the harsh environmental conditions of the mountain ecosystem, which include strong winds and temperatures below 0 C°, and limits the risk of being preyed upon by its main predator the Ethiopian wolf (*Canis simensis*) (Sillero-Zubiri & Gottelli, 1995; Šumbera et al., 2020; Vlasatá et al., 2017; Yalden, 1985). Taken together, the species' key role as ecosystem engineer combined with its limited range in a changing mountain ecosystem, makes it an ideal model organism for investigating the connection between genetic patterns and landscape features, so as to preserve mountain biodiversity and ensure ecosystem functioning.

In the present study, we analysed the spatial genetic subdivision and diversity in the giant root-rat across its distribution range. To achieve this, we analysed both mitochondrial genomes (mitogenomes) and nuclear genomes, and further utilized mitogenomes to investigate the relationship between genetic differentiation and landscape features. We generated complete mitogenomes and low-coverage nuclear genomes from 77 individuals collected across nine sampling localities in the Bale Mountains (Figure 1). We applied two different landscape genetic approaches to evaluate how mitochondrial gene flow of the species is impacted by geographic distance, by vegetation and soil moisture (used as proxies for food and soil availability), and by slope and elevation (used as proxies for topographic barriers). Due to the predominantly below-ground activity and patchy distribution of the giant root-rat, we hypothesise strong genetic subdivision across small spatial scales. Owing to the pronounced heterogeneity of the environment in the Bale Mountains, we hypothesise that genetic structuring is driven by habitat availability, and by topographic structures across the species' range.

2. Materials and method

2.1. Study area

The Bale Mountains in southeast Ethiopia (6º29'N – 7º10'N and 39º28'E – 39º57') represent Africa's largest afro-alpine ecosystem, comprising ~8 % of the continent's area above 3,000 metres above sea level (m a.s.l) (Groos et al., 2021, Figure 1A-C). In order to protect the unique afro-montane and afro-alpine ecosystem of the Bale Mountains, the area above ~3,200 m a.s.l. became a national park in 1970. The Bale Mountains are characterised by two rainy seasons and one dry season per year, with short rains from March to June, long rains from July to October, and a dry season from November to February. The vegetation of the Bale Mountains shows an elevational zonation from moist montane forest (~1,500 - 3,500 m a.s.l.) over ericaceous shrubland and dwarf forest (~3,500 - 4,000 m a.s.l.) to afro-alpine vegetation with open grassland and *Erica* outposts (above 4,000 m a.s.l.). Dwarf-scrub vegetation, such as *Helichrysum* associated with *Lobelia*, is the main plant formation in the afro-alpine vegetation but does not cover the whole area, leaving open spaces for herbaceous plants like *Senecio*, *Alchemilla* or *Salvia* (Miehe & Miehe, 1994; Tallents & Macdonald, 2011)

Characteristic of the Bale Mountains National Park is the afro-alpine Sanetti Plateau, which spans elevations from approximately 3,800 m a.s.l, to 4,377 m a.s.l. at the peak of the mountain Tullu Dimtu (Figure 1C). Large parts of the plateau were glaciated during the Late Pleistocene, between 42,000 to 16,000 years ago (Groos et al., 2021). The plateau is bounded by several outlet valleys in the north and the east with slopes that are covered by dense, shrubby *Erica* vegetation and by congealed lava flows at its northwestern margins. These topographic structures distinguish the plateau from the northern region of the national park, which is ~300 - 500 m lower in elevation and comprises broad valleys and plains with afro-alpine vegetation (Miehe & Miehe, 1994). In comparison to the plateau, the north has higher moisture availability and milder temperatures.

148 **2.2 Sampling**

149 We collected tissue samples from 77 live giant root-rat individuals at nine localities across the Bale
150 Mountains National Park, covering the distribution range of the species (Figure 1C, supporting
151 information Table S1). The sampling localities were distributed across the two topographically distinct
152 regions in the national park, in the north (localities N1-N3) and in the south (localities S1-S6). The
153 southern localities are scattered across the centre and south of the Sanetti Plateau. Localities sampled
154 in the north of the plateau lie at a lower elevation (~3,500 m a.s.l) than localities sampled in the south
155 (~3800 - 4000 m a.s.l.). Sampling localities between regions were separated by 15.3 to 28.3 km, and
156 localities within regions were separated by 2.6 km to 16.0 km.

157 We captured 7-9 giant root-rat individuals per locality (except locality S4 with n=1). The samples
158 were collected in January and February in two consecutive years (2020, 2021) under the permit of the
159 Ethiopian Wildlife Conservation Authority. Individuals were caught with snare traps that were
160 monitored by the capture team at all times to guarantee no harm to the animals. A ~0.5 cm^2 piece of
161 skin from the hind leg was cut with sterilised scissors and stored in 96% ethanol or DNAgard® for blood
162 and tissue (Biomatrica, Inc.) for genomic analyses. After sterilising the wound, the animals were
163 immediately released back into their burrow systems.

164

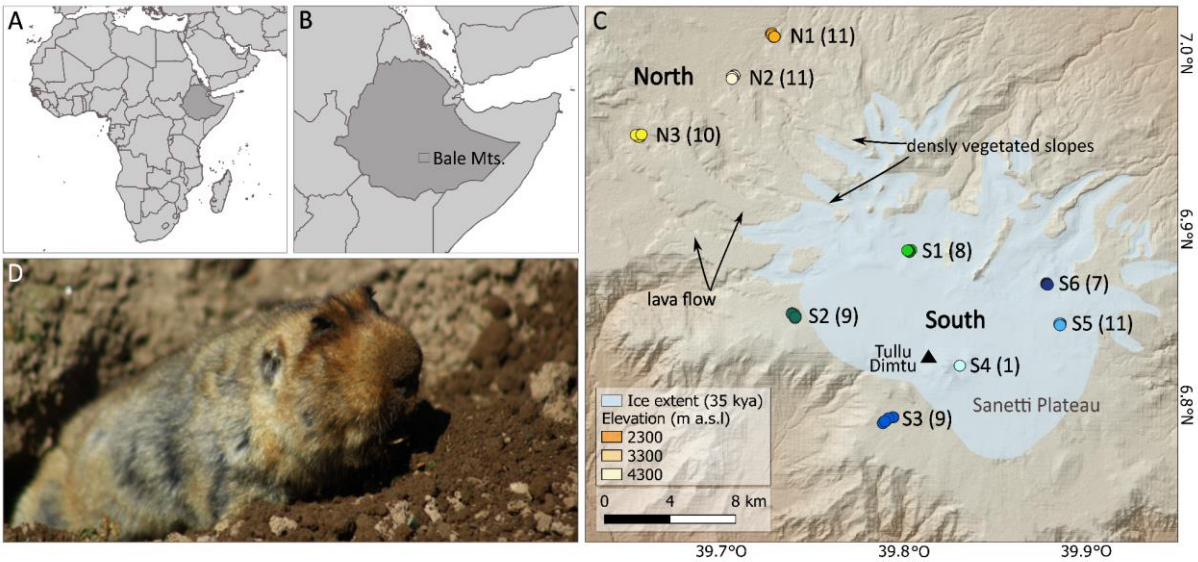

Figure 1: Sampling localities of giant root-rats within Bale Mountains National Park, Ethiopia. A) Map of Africa showing Ethiopia in dark grey; B) Map of Ethiopia indicating location of Bale Mountains National Park, C) Map of the nine sampling localities from two distinct geographic regions. The north (~3,500 m above sea level [m a.s.l]), and south (~3,800-4,000 m a.s.l, Sanetti Plateau) are separated by steep slopes covered with dense *Erica* thickets and congealed lava flows. Sample size of each locality is indicated in brackets. Tullu Dimtu is the highest peak in the Bale Mountain National Park at 4,377 m a.s.l., and is indicated with a filled triangle. Region with light blue shading indicates the glacial extent within Bale Mountains National Park ~35±7.1 thousand years ago (kya) (Groos et al., 2021; Ossendorf et al., 2019); D) Burrowing giant root-rat, photography by V. Reuber.

2.3 Laboratory analyses

We extracted DNA from the tissue samples using the Qiagen DNeasy® Blood and Tissue Kit following the manufacturer's protocol (Qiagen Ltd.). 60 of the samples were processed in-house in the modern DNA labs at Globe Institute, University of Copenhagen. The DNA concentration of the extracts was measured using QubitTM dsDNA HS (Invitrogen). After quantification, we diluted the extracts to a concentration of 6 ng/µl in a total volume of 50 µl. DNA was sheared to ~400 base pair (bp) fragment lengths using the Covaris M220 ultrasonicator. We built DNA fragments into an Illumina library following the protocol from Carøe et al., (2018) and double-indexed them using AmpliTaq Gold Polymerase (ThermoFisher) during the indexing PCR step. Index PCR reactions were performed in 100 µl, using 1x PCR buffer, 2.5 mM of MgCl (25 mM), 0.2 mM of dNTPs (25 mM), 0.2 µM of index primer mix (10 µM), and 0.1 U/ µl of polymerase (5 U/µl). PCR cycling conditions were 95 °C for 10 min; 10 -

185 18 cycles of 95 °C for 30 s, 50 °C for 30 s and 72 °C for 1 min followed by 72 °C for 5 min. The number
186 of cycles for the index PCR was determined from qPCR analysis. Post-amplification, libraries were
187 purified using SPRI beads as in Carøe et al., (2018). The purified indexed libraries were quantified on a
188 QubitTM dsDNA HS (Invitrogen), and quality-checked on either an Agilent 2100 Bioanalyser or an
189 Agilent Fragment AnalyzerTM. Libraries were pooled equimolarly and sequenced on an Illumina
190 NovaSeq 6000 using paired-end (PE) 150 bp technology (Novogene Europe, http://en.novogene.com).
191 For the remaining 17 samples, DNA was extracted and processed to libraries by Novogene and
192 sequenced on a NovaSeq 6000, using paired end 150 bp technology.

193 **2.4 Data generation of mitochondrial and nuclear DNA**

194 We trimmed adapters and removed reads shorter than 30 bp for each individual using skewer v0.2.2.
195 (Jiang et al. 2014). We merged overlapping paired-end reads using FLASHv1.2v11 (Magoč & Salzberg,
196 2011) with default parameters. We mapped both merged and unmerged reads to the hoary bamboo
197 rat (*Rhizomys pruinosus*) nuclear genome (Genbank accession: VZQC00000000.1; Guo et al., 2021)
198 which is the nearest relative of the giant root-rat with an available genome, combined with the giant
199 root-rat mitogenome (Genbank accession: MW751806; Reuber et al., 2021). We used BWA v0.7.15 (Li
200 & Durbin, 2009) utilising the mem algorithm and default parameters. We parsed the alignment files,
201 and removed duplicates and reads of mapping quality score <30 using SAMtools v1.6 (Li et al., 2009).
202 We built consensus mitogenomes from each individual using a majority rules approach (-doFasta 2) in
203 ANGSD v0.921 (Korneliussen et al., 2014) only considering bases with a base quality score greater than
204 30 (-minq 30), reads with a mapping quality score greater than 30 (-minmapq 30), and sites with at
205 least 10x coverage (-minInddepth 10). The mitogenomes are available under GenBank accessions
206 OQ207545 - OQ207620.

207 **2.5. Genetic subdivision**

208 2.5.1 Mitochondrial DNA analysis

209 *Haplotype network*

210 The mitogenomes were aligned with Mafft v.7.392 (Katoh & Standley, 2013). We constructed a
211 median-joining haplotype network to investigate the relationships among the 77 mitogenomes using
212 the software PopArt v.1.7 (Leigh & Bryant, 2015).

213

214 *Phylogenetic analysis*

215 We constructed a Bayesian phylogeny with the 48 mitogenome haplotypes identified in the network
216 analyses, using MrBayes v.3.2.7a (Ronquist & Huelsenbeck, 2003). We used the GTR + I + G model of
217 evolution, which was defined as the best model with PartitionFinder v. 2.1.1 (Lanfear et al., 2017) prior
218 to the analysis. The MCMC algorithm was run twice with four chains of 10 million generations, sampled
219 every 1,000 generations and with a 10 % burn-in. The trees were combined following the majority-rule
220 consensus approach, to assess the posterior probability of each clade. The resulting tree was visualised
221 in FigTree v.1.4.4 (http://tree.bio.ed.ac.uk/software/figtree/; supporting information Figure S1).

222

223 *Fixation statistics and AMOVA*

224 We calculated the pairwise differentiation between eight of the nine sampled localities (omitting S4 as
225 n=1) with the F_{ST} -estimator of the software Arlequin v. 3.5.2.2 with 10,000 permutations (Excoffier &
226 Lischer, 2010); *p*-values of F_{st} estimates were adjusted using the Bonferroni correction (Rice, 1989),
227 controlling for a false-positive discovery rate (R Core Team, 2021). Additionally, we conducted a
228 hierarchical analysis of molecular variance (AMOVA), also in Arlequin, with localities grouped into their
229 provenance in the regions north and south (Figure 1C).

230 2.5.2 Nuclear DNA analysis

231 We investigated population subdivision of the nuclear data using principal component analysis (PCA)
232 and admixture proportion analysis. We generated genotype likelihoods in ANGSD (Korneliussen et al.,
233 2014) for all individuals using the following filters and parameters: call genotype likelihoods using the
234 GATK algorithm (-GL 2), output a beagle file (-doGlf 2), only include reads with mapping and base
235 qualities greater than 30 (-minmapQ 30 and -minQ 30), only include reads that map to one location
236 uniquely (-uniqueonly 1), a minimum minor allele frequency of 0.05 (-minmaf 0.05), only call a SNP if
237 the p-value is greater than $1e^{-6}$ (-SNP_pval 1e-6), infer major and minor alleles from genotype
238 likelihoods (-doMajorMinor 1), only include sites if at least 40 individuals are covered (-MinInd 40),
239 remove scaffolds shorter than 100 kb (-rf), and remove secondary alignments (-remove_bads 1). To
240 compute the PCA, we constructed a covariance matrix from the genotype likelihoods using PCAngsd
241 v0.98 (Meisner & Albrechtsen, 2018). Admixture proportions were calculated using the same genotype
242 likelihoods with NGSadmix (Skotte et al., 2013). We ran NGSadmix specifying K=2 and K=3. To evaluate
243 the reliability of the NGSadmix results, we ran each *K* up to 100 times independently. If we retrieved
244 consistent log-likelihoods from at least two independent runs, the corresponding K was considered
245 reliable.

246 To estimate levels of differentiation among localities, we computed F_{ST} from a consensus haploid
247 call file created using ANGSD (-dohaplocall 2) and the same filtering parameters as the PCA and
248 admixture proportions above. We calculated the F_{ST} using an available python script
249 https://github.com/simonhmartin/genomics_general/blob/master/popgenWindows.py) and
250 specifying a window size of 1Mb, and a minimum number of sites per window as 1,000 bp.

251

252 *Gene flow*

253 The mitogenomes of two individuals (WM07 from locality S1 and GG01 from locality S6) grouped with
254 individuals from the north in the haplotype network and phylogeny. We therefore used D-statistics

255 (also known as ABBA/BABA, Durand et al., 2011) to test whether the results were driven by ancient
256 gene flow between regions north and south, or by incomplete lineage sorting. We tested several
257 topologies [[H1, H2], H3], with branch H1 being one of the two putative introgressed individuals, and
258 branches H2 and H3 being individuals from one region north or south, or one from each region. A
259 negative D-score illustrates a closer relationship between H1 and H3 than H2 and H3, while a positive
260 D-score indicates that branches H2 and H3 are more closely related than H1 and H2. This setup can
261 also be used to uncover population subdivision, as the incorrect input topologies would lead to
262 elevated D-scores due to more recent common ancestry, as opposed to gene flow (Westbury et al.,
263 2018).

264 We performed the D-statistic tests using a random base-call approach in ANGSD (-doAbbababa 1).
265 We implemented the same filtering approach as for the above analyses but only included scaffolds >1
266 megabase (Mb) in size, a block size of 1 Mb (-blocksize 1000000), and the hoary bamboo rat (*Rhizomys*
267 *pruinosus*, GenBank accession VZQC00000000.1, Guo et al., 2021) as the ancestral state/outgroup (-
268 anc). To assess the significance of our results we used a block jackknife test with the script jackKnife.R
269 which is available with the ANGSD tool suite.

270 **2.6 Diversity**

271 Based on the mitochondrial genomes, we calculated nucleotide diversity (π) per region, and separately
272 for eight of the nine localities using DnaSp v.6 (omitting S4 as n=1) (Rozas et al., 2003). We tested
273 differences in nucleotide diversity between the two geographic regions, and among localities using
274 genetic_diversity_diffs v. 1.0.3 (Alexander, 2017).

275 The python script used to calculate nuclear F_{ST} above simultaneously computes nucleotide
276 diversity per region and per locality. To test for significant differences in levels of nucleotide diversity
277 between regions and between localities, we used a Welch-test (unpaired t-test), accounting for
278 unequal variance.

2.7 Landscape genetic analysis

We applied two landscape genetic approaches to investigate the effects of landscape features on the observed genetic differentiation between localities based on F_{ST} estimates of the mitogenomes. We exclusively used mitogenomes due to their higher mutation rates and lack of recombination compared to nuclear genomes, which result in faster responses to environmental changes and increased resolution (Avise, 2000; Birky et al., 1983). The limited number of sampling localities prevented us from analysing the north and south regions separately.

We selected four environmental variables (vegetation, soil moisture, slope, elevation), which were based on satellite-based remote sensing data, as predictors for genetic differentiation of the giant root-rat. For vegetation and soil moisture, we used observations from satellite Sentinel-2, captured on an almost cloud-free day on December 15, 2017, and derived from the USGS Earth Explorer repository. We used the red, green, blue, red and near infrared bands of from the Sentinel-2 observations and with those computed raster layers of the Normalised Differentiation Vegetation Index (vegetation index) and Land-Surface Water Index (soil moisture index, for details see Wraase et al., 2022) using the Rtoolbox, as proxies for food and soil availability for giant root-rats (Sillero-Zubiri et al., 1995; Šklíba et al., 2017; Yaba et al., 2011; Yalden & Largen, 1992). To determine whether topographic structures act as barriers for burrowing giant root-rats, we included the variables slope and elevation in our analysis. Raster layers for slope and elevation were obtained from a Shuttle-Radar-Topography-Mission digital elevation model from the USGS Earth explorer (www.earthexplorer.usgs.gov). The generated raster layers of all four environmental variables had a 30 x 30 m resolution and were cropped on extent 567910.0, 605990.0, 738620.0, 778750.0. Our analyses were conducted in R environment version 4.2.1 (R Core Team, 2021).

Partial Mantel tests

303 Using partial Mantel tests, we analysed if the genetic differentiation between eight of the nine
304 sampling localities (omitting S4 as n=1) was correlated with geographic distance, vegetation, soil
305 moisture, slope and elevation (see above). Therefore, we constructed distance matrices. The genetic
306 distance matrix was generated by linearizing the pairwise genetic differentiation estimates between
307 localities, i.e the F_{ST} -estimates ([F_{ST} /(1- F_{ST})]; Rousset, 1997). The geographic distance matrix was
308 calculated in Euclidean distances and log-transformed to linearize the relationship with genetic
309 distance. For each environmental variable, we extracted their values from the computed raster layers
310 at the coordinates of the sampling localities and therewith generated the environmental distance
311 matrices. We then applied a pairwise reciprocal causal modelling approach. Reciprocal causal
312 modelling compares partial Mantel tests of a focal environmental model, removing the influence of a
313 competing, alternative model (Cushman et al., 2006; Cushman & Landguth, 2010). In this approach,
314 the correlation between one environmental distance matrix and genetic distance is controlled by a
315 second matrix (e.g. focal model: genetic distance~geographic distance|elevation distance) and in a
316 next step, both environmental distance matrices are interchanged (e.g. alternative model: genetic
317 distance~elevation distance|geographic distance). In that way, we were able to account for high
318 correlation among matrices (Cushman et al., 2006; Cushman & Landguth, 2010). To assess which of
319 the two models explains genetic distance better, the relative support of the focal and alternative model
320 was calculated by estimating the difference between the correlation values of the two models. If the
321 difference in correlation factors was positive, we assumed that the focal hypothesis was correct. The
322 partial Mantel tests were performed with 9,999 permutations in the vegan R package v.2.6-4. (Oksanen
323 et al., 2020).
324
325 *Raster layer optimization framework to generate resistance surfaces*
326 We used a raster layer optimization framework developed by Peterman et al. (Peterman, 2018;
327 Peterman et al., 2014), to further identify landscape features that explain mitochondrial genetic

328 differentiation, using the R package ResistanceGA (Peterman, 2018). In this framework, the raster
329 layers of the environmental variables (see above) were transformed into resistance surfaces, with the
330 ResistanceGA package utilising a genetic algorithm from the GA R package (Scrucca, 2013). A resistance
331 surface is a spatial layer that assigns values to each grid in the raster layer of the selected
332 environmental variable. Those values are used to estimate the cost of dispersal and mirror to what
333 extent the selected variable hinders or facilitates the connectivity of a species between two localities
334 (pairwise resistance distances). Thereby, there are no *a priori* assumptions about the relationship
335 between the environmental variable and the species' dispersal characteristics. The genetic algorithm
336 in the optimization framework is used to maximise the relationship between the resistance distances
337 of each raster layer, and the pairwise genetic differentiation (F_{ST}) between localities. The process of
338 generating resistance surfaces is repeated, and in every iteration, the resistance distances are fitted
339 against the genetic distances in a mixed effect model, until the objective function, the AIC (Akaike's
340 information criterion; Akaike, 1974) of the mixed effect model does not improve further. The mixed-
341 effect models are conducted using a maximum likelihood population effect parameterization to
342 account for the non-independence of the predictor variables and to account for spatial autocorrelation
343 (Clarke et al., 2002; Peterman et al., 2014; Shirk et al., 2018). This iterative process works towards
344 identifying the best-fit landscape resistance surface.

345 In our optimization framework, we used a single surface optimization approach, where the
346 resistance surfaces of the raster layers of each selected environmental variable (i.e. vegetation index,
347 soil moisture index, slope and elevation) were optimised individually, using eight transformation
348 functions (Monomolecular and Ricker functions) and the default parameters (Peterman, 2018). In this
349 step, the pairwise resistance distance between localities was estimated by assuming that individuals
350 can use several paths to disperse. Resistance distances were generated with the *costDist* function
351 implemented in the ResistanceGA package and movements between localities were allowed in eight
352 directions during resistance distance calculation. Because Euclidean distance is incorporated in the

resistance distances, it was not included as an additional variable. In the optimization process, the mixed-effect models were calculated, fitting the pairwise genetic differentiation as a response against the resistance distances as single fixed effects, using the AIC for model evaluation and including sampling localities as a random effect to account for spatial autocorrelation. We did two independent optimization runs to confirm convergence across runs. The run containing the mixed-model with the greatest log-likelihood value is presented in the results section (Table 1). After the optimization, we used bootstrap model selection with 75% of the samples and 10,000 iterations. The bootstrap model selection refits the mixed-effect models and calculates fit statistics for each model, showing the average AIC and percentage each resistance surface has been selected as a top rank model across all bootstrap iterations (Peterman, 2018).

3. Results

We generated complete mitogenomes from all 77 giant root-rat individuals, with a depth of coverage ranging between 24.94x and 383.22x, and a length of 16,646 bp. For the nuclear genomes, we obtained coverages ranging from 0.12x to 0.77x (supporting information Table S2).

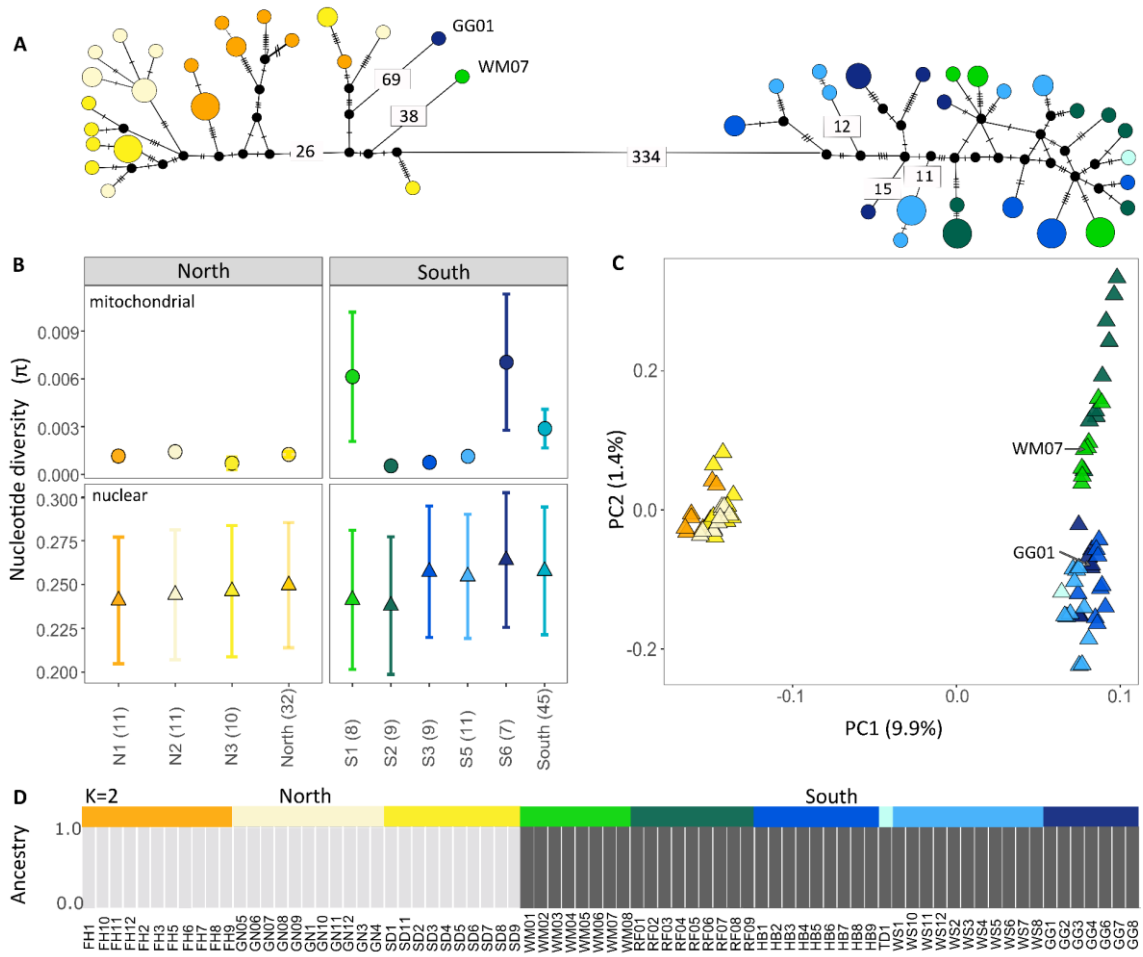

Figure 2: Patterns of genetic diversity and subdivision of giant root-rats across their range. A) Network of the 48 mitochondrial haplotypes present among the 77 sampled individuals. Each circle represents a haplotype, and the relative size of each circle represents haplotype frequency. Numbers on branches show the number of segregating sites between haplotypes for >10. Black dots indicate intermediate haplotypes not present in the data. Distances between haplotypes are not to scale. B) Diversity levels within the sampled localities and subpopulations based on mitogenomes (circles) and nuclear data (triangles). Sample sizes are shown in brackets. C) PCA based on 77 low-coverage nuclear genomes. The percentage of the diversity of each principal component is shown in brackets. D) Ancestry proportions based on the nuclear data for K=2, with each vertical bar representing an individual.

3.1 Genomic analysis

Haplotype network and phylogeny

Our 77 sampled giant root-rat individuals comprised 48 haplotypes, with no haplotypes shared among localities (Figure 2A). The haplotype network and phylogeny of the mitogenomes revealed two geographically separated and well-supported groups; one group comprising all samples collected in

382 the north, with the inclusion of individuals WM07 and GG01 from the south, and one group comprising
383 all other samples from the south (supporting information Figure S1). In the network, we identified 574
384 segregating sites among individuals, and the northern and southern haplogroups were separated by
385 334 segregating sites (Figure 2A). The north contained 21 haplotypes (32 individuals) and the south
386 contained 27 haplotypes (45 individuals). Within the north, we identified two distinct, well-supported
387 genetic clades, N_A and N_B (supporting information Figure S1). Clade N_A comprised six individuals (five
388 haplotypes) from localities N1-N3. Individual GG01 from locality S6 was basal to the clade. Clade N_B
389 comprised the remaining individuals from the north with individual WM07 from the south at basal
390 position. We did not identify any spatial genetic structuring in the south.

391 The AMOVA yielded a high level of between-region variation when the eight localities (omitting
392 S4 with n=1) were grouped into north and south (89.50 %, $p < 0.01$). Within each region, the variation
393 was higher within localities (9.27 %) than among localities (1.24 %).

394

395 *Principal component analysis and admixture proportions*

396 We identified two main groups in the nuclear data, in agreement with the mitochondrial findings
397 (Figure 2). In the PCA, individuals from the north separated from the individuals from the south, with
398 almost 10% of the variation explained on the first principal component. The southern group showed a
399 slight separation on the second component, with the more central localities S1 and S2 segregating
400 from the localities further southeast, with 1.4 % variation explained (Figure 2C). The division of the
401 data into north and south was also evident in the admixture analysis of K = 2 (Figure 2D). The admixture
402 analysis did not converge with K = 3, suggesting K = 3 did not reliably fit the data.

403

404 *Gene flow*

405 To investigate the origin of the mitochondrial lineages, present in individuals WW07 and GG01, which
406 were more closely related to the northern haplogroup than the south (Figure 2A), we tested for ancient

407 gene flow using the nuclear data. Using the topology [[WM07, south], north], we found most
408 comparisons to have a D-score around 0 and a Z-score<|3|, indicating that WM07 and all individuals
409 from the south were equally related to the northern individuals (Figure 3). We found positive D-scores
410 (Z-score>3) when using the topology [[WM07, north], north], demonstrating a closer relationship
411 between individuals from the north with each other than with WM07, which agrees with their more
412 recent common ancestry and the basal position of WM07 in the phylogenetic tree (supporting
413 information Figure S1). We found qualitatively the same results when we investigated the relationship
414 of GG01 (sampled in locality S6) with individuals from the north and south (Figure 3). Hence our
415 analysis did not support that the mitochondrial lineages in WM07 and GG01 were the result of recent
416 gene flow between north and south.

417

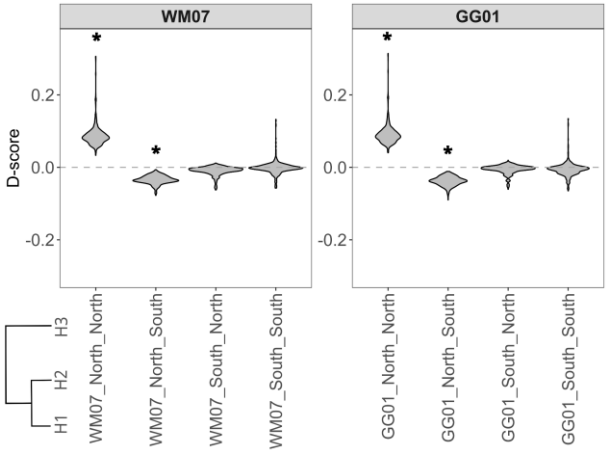

418
419
420 Figure 3: Analysis of signals of gene flow between individuals WM07 from locality S1 and GG01 from locality S6
421 and their source group in the south, using D-statistics. Negative D-scores suggest gene flow or recent common
422 ancestry between H1 and H3 relative to H2 and H3, while positive D-scores suggest gene flow or recent common
423 ancestry between H2 and H2 relative to H1 and H3. Statistical significance is indicated by asterisks (*) next to
424 scores, when |Z| greater than 3 (supporting information Figure S2), determined by a one-sample Wilcoxon
425 signed rank test.
426

427 *Genetic differentiation among localities*

428 Investigating pairwise genetic differentiation between localities, we found that F_{ST} - estimates were
429 higher between regions than within regions, at both the mitogenome and nuclear level (Figure 4). For

the mitogenomes, pairwise differences between localities of different regions ranged from 0.82 to 0.97 and were much higher than within regions, where values ranged from 0.09 to 0.29.

For the nuclear data, pairwise F_{ST} - estimates between localities from different regions ranged from 0.04 to 0.06 and were higher than values between localities within regions, which ranged from 0.01 to 0.02 (Figure 4).

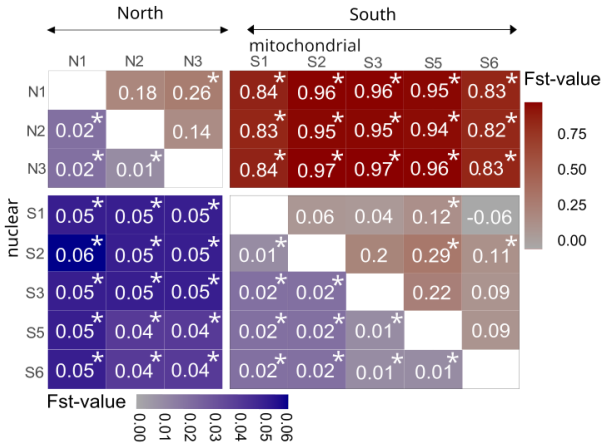

Figure 4: Levels of genetic differentiation between the sampled giant root-rat localities from the north and south of Bale Mountains National Park. Mitochondrial (red, above diagonal) and nuclear (blue, below diagonal) F_{ST}-estimates. * in cells indicates significant differences (*p*-values < 0.05), derived by permuting haplotypes between localities for mitochondrial data and by applying a one-sample t-test on F_{ST} -values for the nuclear data.

Diversity

We estimated levels of diversity for each region, and for each locality (omitting S4 as n=1). For the mitogenomes, diversity in the south (π = 0.003 ± 0.0002) was significantly higher than in the north (π = 0.001 ± 0.001, $p < 0.05$; Figure 2B), which reflected the presence of the divergent mitochondrial lineages in individuals WM07 and GG01 from localities S1 and S6 (Figure 2A). Thus, this was also apparent in localities S1 and S6 having the highest diversity levels, with S6 showing significantly differentiated levels of diversity ($p < 0.05$) and S1 showing marginal significant differentiation ($p > 0.05 < 0.1$, supporting information Table S3) to the remaining localities in the south.

Based on the nuclear data, we also observed significantly higher diversity in the south (π = 0.257 ± 0.0364) than in the north (π = 0.249 ± 0.0357, $p < 0.05$; Figure 2B). Among localities in the south, the

451 two central localities S1 and S2 had lower diversity levels than the localities sampled further to the
452 southeast (S3, S5, S6). All localities had significantly differentiated levels of diversity ($p < 0.05$,
453 supporting information Table S3).

454 **3.2 Landscape genetics**

455 We used a reciprocal causal modelling approach with partial Mantel tests to relate genetic
456 differentiation to the environmental distance matrices of the selected variables (vegetation index, soil
457 moisture index, slope and elevation). Analysing levels of differentiation estimated for each region we
458 found that elevation was the strongest model. Elevation was significantly related to genetic
459 differentiation in all partial Mantel tests, regardless of the second environmental distance matrix
460 controlling elevation (supporting information Table S4 A). Further, elevation showed the strongest
461 relative support; all relative correlation values were positive, after the effect of the other
462 environmental models were removed (supporting information Table S4 B). Geographic distance
463 showed a significant relation with genetic differentiation when controlled by vegetation index, soil
464 moisture index or slope, but was non-significant and the relative correlation value was negative, when
465 controlled by elevation. We could not find significant effects of vegetation, soil moisture or slope on
466 genetic differentiation; all variables had non-significant Mantel correlation values, showing the least
467 support in the reciprocal causal modelling matrix (supporting information Table S4).

468 The raster layer optimization approach revealed that slope and elevation were the best-fitting
469 models for explaining genetic differentiation. Slope was selected as top model in 71%, and elevation
470 in 29% of the times across 10,000 bootstrap iterations (Table 1). The average weight from the
471 bootstrap analyses supported geographic distance as a driver for genetic differentiation, while the
472 parameters rank, AIC, maximum likelihood and R^2 suggested slope and elevation as the best models
473 (Table 1). The the response curve of the optimised resistance surface showed that the resistance costs
474 increased with increasing slope (supporting information Figure S3 C). As in the partial Mantel tests, we

could not identify a contribution of the vegetation index or soil moisture index to genetic differentiation (Table 1).

Table 1: Model selection results for linear mixed-effect models, testing the effect of resistance distances (dispersal costs based on environmental condition) on levels of mitochondrial genetic differentiation (F_{ST}) in the giant root-rat. The parameters were calculated based on 10,000 bootstrap iterations using a random resampling of 75% of the sampled populations. Frequency top-model percentage, higher average weight and log-likelihood (LL), and lower average rank indicate the best supported models.

Resistance distance matrix	**Average AIC**	**Average R^2m**	**Average LL**	**Average weight**	**Average rank**	**Frequency top model (%)**
Slope	-16.61	0.92	12.31	4.8E-05	1.36	70.87
Elevation	-10.29	0.86	9.15	0.004	2.88	29.13
Vegetation	-7.16	0.78	7.58	4.0E-07	3.19	0
Soil moisture	-6.26	0.78	7.13	1.2E-06	3.57	0
Distance	-4.20	0.65	4.10	0.990	4.00	0

4. Discussion

Using complete mitochondrial genomes and low-coverage nuclear genomes from 77 giant root-rat individuals, we uncovered a clear subdivision of localities in the north and the south of the species range in the Bale Mountains, Ethiopia. Landscape genetic analysis identified topographic barriers such as the steep slopes and elevation differences between the two regions as the main drivers of population subdivision. Within regions, we did not identify any clear spatial structuring, suggesting a high level of gene flow when topographic barriers are absent.

Genetic subdivision between regions

The significant north and south geographic subdivision in the mitochondrial and nuclear genomes, was evidenced, for instance, by a high number of substitutions separating the divergent mitochondrial lineages present in each region, or by the nuclear PCA analysis (Figure 2, supporting information Figure S1). However, two giant root-rat individuals sampled in the south were mitochondrially more closely related to their northern counterparts than their source region, which may indicate ancient gene flow. Despite their closer relationship, both had a large number of substitutions distinguishing them from

498 the rest of the northern individuals, suggesting that ancestral mitochondrial lineages may be retained
499 in those two individuals that are also present in the north - a remnant of their shared evolutionary
500 history. The phylogeny indicated these two southern individuals as basal to each of two distinct
501 haplogroups found in the north, suggesting the lineages were derived from two distinct divergence
502 events. Ancient lineage retention in the south was supported by our nuclear analysis, which found no
503 evidence of recent or past gene flow between north and south (Figures 2D, 3).

504 The presence of genetically distinct subpopulations may be attributed to long-lasting extrinsic
505 barriers, which prevent genetic exchange between them (Avise, 2000; Bryja et al., 2010). Slope and
506 elevation were identified as the primary drivers of genetic differentiation in our landscape analysis,
507 and in combination they presumably cause the genetic subdivision between regions (Table 1,
508 supporting information Table S4), similar to what has been observed in other fossorial rodents such as
509 the Brazilian tuco tuco of the dunes (*Ctenomys flamarioni*), or the common water vole (*Arvicola*
510 *terrestris*) (Berthier et al., 2005; Fernández-Stolz et al., 2007). The south comprises the Sanetti Plateau,
511 which is ~300 – 500 m higher in altitude than the northern region (Figure 1C) and the plateau margins
512 northwards are characterised by broad valleys with steep slopes covered by dense *Erica* thickets. In
513 addition to the slopes which themselves act as a barrier, the *Erica* thickets may further limit the
514 dispersal of the species (Miehe & Miehe, 1994; Yalden, 1985). Giant root-rats are adapted to open
515 grasslands with low vegetation and avoid dense shrubs such as *Erica*, likely due to the difficulties of
516 burrowing in woody ground and the absence of food-plants. Additionally, the plateau is bounded by
517 congealed lava flows of unknown age to the northwest. These barriers to dispersal and the fossorial
518 lifestyle of the giant root-rat limiting the species' ability to traverse pronounced topographic
519 structures, presumably caused the strong genetic subdivision of the species. Our landscape genetic
520 result is in agreement with recent satellite-based mapping of the giant-root rat's distribution, which
521 found that the texture of the landscape is the most critical factor in explaining the species' range
522 (Wraase et al., 2022).

In addition to slope and elevation, the pronounced subdivision observed in giant root-rats may also have been reinforced by glacial extents during the Late Pleistocene. The Bale Mountains are currently ice-free, but the Sanetti Plateau, the south region, was glaciated between ~42,000 to 16,000 years ago (kya) (Figure 1C; Groos et al., 2021; Ossendorf et al., 2019). Except for this last glacial extent, exposure ages of moraines in the valleys in the northwestern part of the plateau (up to ~100 kya), and stone stripes close the mountain Tullu Dimtu (up to ~360 kya) could be interpreted in favour of earlier glacial periods (Groos et al., 2021). Possibly, giant root-rat individuals in the south were pushed towards the outer margins of the plateau by the glaciers, which increased the separation to the individuals in the north. As the glaciers retreated, colonisation of the central plateau from a more southern Late Pleistocene refugium may explain the significantly lower diversity in the central localities (S1 and S2) in comparison to the south eastern ones (S3, S5, S6, supporting information Table S3). This would be in agreement with the often-proposed hypothesis that populations of mammals exhibit reduced genetic diversity on recently deglaciated land (e.g. Hewitt, 1996, 2004). The glacial extent in the north and northwestern valleys of the plateau margins persisted until ~16,000 years ago, while the ice shield on the plateau around Tullu Dimtu was smaller in extent already ~20,000 years ago (Groos et al., 2021).

Although vegetation and soil moisture were previously identified as essential factors influencing the local abundance of giant root-rats (Asefa et al., 2022; Šklíba et al., 2017), our study did not indicate any effect on genetic differentiation (Table 1), suggesting these factors play less of a role in hindering gene flow at the range-wide scale. However, the spatially coarse vegetation and soil moisture indices used in our analysis may not fully capture the highly specific food and soil requirements of the giant root-rat. Their primary food resource is *Alchemilla* (Yaba et al., 2011). The vegetation index, which is based on remotely-derived satellite data, may not distinguish its spectral signal from other non-preferred plants (Wraase et al., 2022). Additionally, the giant root-rat requires soil layers of approximately 50 cm in depth to engineer burrow systems and for thermoregulation (Sillero-Zubiri et

al., 1995; Šumbera et al., 2020), and while soil depth and moisture are likely correlated (deeper soil can store more water, Tromp-van Meerveld & McDonnell, 2006), soil moisture as a proxy for soil availability may not capture areas of sufficient soil depth. The vegetation and soil moisture indices were derived from a Sentinel-2 scene captured in December, just after the rainy season. During this period, vegetation is still lush and green and the soil is moist across large parts in the Bale Mountains National Park, and this thus might not fully reveal the specific habitat requirements (related to its preference for moorlands and wet grasslands with good soil depth) of the giant root-rat at that time of the year.

Gene flow within regions

We observed a lack of structuring among localities within both regions. Levels of differentiation were low, with nuclear F_{ST} - estimates of 0.01-0.02 within regions, which is considered as weak differentiation for nuclear data (Figure 4; Weir & Cockerham, 1984; Wright, 1978). This indicates high level of dispersal and gene flow across distances of at least 16 km, which was the maximum distance between two sampling localities within regions. The ability of giant root-rats to disperse across such relatively large distances was in contrast to our expectations; giant root-rats are fossorial, solitary and territorial. We had expected this, in combination with the heterogeneity in soil structure and food availability across its range, would lead to stronger genetic structuring at small spatial scales, similar to what has been observed in other fossorial rodents (Mapelli et al., 2012; Schweizer et al., 2007). Although direct observations for this are still lacking, the limited substructuring within regions and the large dispersal distances suggest that giant root-rats can disperse aboveground and for relatively large distances. In fact, giant root-rats show morphological adaptations to surface activity, in that their eyes are situated dorsally on the head, which allows them to detect predators in open habitats (Yalden, 1985). In support of our findings, radio tracking has evidenced the dispersal of a giant root-rat individual over a distance of up to 270 m within a span of two days; the tracked individual traversed

across damp soil, suggesting it did not disperse underground (Šklíba et al., 2020). Aboveground dispersal has also been documented in other fossorial, solitary rodent species, such as blind mole-rats (*Spalax microphthalmus*; Zagorodniuk et al., 2018) and Tibetian plateau zokors (*Eospalax fontanieri*; Chu et al., 2021). Even in strictly subterranean African mole-rats, long-distance dispersal is not precluded (*Fukomys damarensis*, Bathyergidae; Finn et al., 2022). For giant root-rats, aboveground dispersal attempts could be triggered by decreasing food supply, the absence of sexual partners, or the presence of competitors (Šklíba et al., 2020; Zagorodniuk et al., 2018). Also, the behaviour may circumvent the patchy availability of suitable habitats and small home-ranges, maintaining gene flow and limiting genetic structuring across small spatial scales.

Dispersal events in the giant root-rat may be male-dominated, as it has been observed in tuco tucos (*Ctenomys talarum* and *C. australis*; Cutrera et al., 2005; Mora et al., 2010), Chinese zokor (*Eospalax fontanierii*, Zhang, 2007), giant mole-rats (*F. mechowii*; Kawalika & Burda, 2007), and arvicoline rodents (Le Galliard et al., 2012). While sex-specific dispersal has not been studied in the giant root-rat yet, the observation of males being more frequently involved in dispersal attempts compared to females (Šklíba et al., 2020) and that microsatellite analysis also indicate that males disperse for longer distances (Dovičicová et al. in prep.) suggests that this type of dispersal may be prevalent in the species.

Our nuclear data did suggest slight subdivision in the south, with localities in the central part of the plateau (S1, S2) being more differentiated from localities in the southeast (S3-S6; Figure 1C). This was evidenced by increased F_{ST} in their pairwise comparisons and their segregation on the second principal component on the PCA (Figure 2C, D). Although overall differentiation among localities in the south were low, this pattern may reflect topographic features; the mountain Tullu Dimtu, the highest peak in the Bale Mountains National Park with 4,377 m a.s.l., is located close to localities S3 and S4, and may hinder gene flow (Figure 1C).

Conservation implications

Through landscape genetic analysis, we identified the drivers of population subdivision between north and south to be topographic barriers in the form of slope and elevation. While the species is capable of dispersing locally, our findings suggest that giant root-rats in the north and south must be considered separately when developing conservation strategies, as there is no opportunity for dispersal and gene flow between them. Giant root-rat impact their surrounding environment as ecosystem engineers and primary prey for the endangered Ethiopian wolf, which underscores the importance of their persistence (Sillero-Zubiri & Gottelli, 1995; Šklíba et al., 2017). Already, the giant root-rat is believed to have a small census size due to its limited distribution range (although no census estimate is available), and is listed as endangered by the IUCN (Lavrenchenko & Kennerley, 2016). The potential for reduction of the species' distribution range due to increasing human activities in the form of expanding livestock grazing and human settlements in the Bale Mountains, could harm the species' persistence with negative consequences for the overall ecological balance in the region (Gashaw, 2015; Mekonen, 2020; Stephens et al., 2001). Our study yields some key insights for planning future conservation strategies for the species and highlights the value of genomic data in expanding our understanding of the population dynamics and environmental features that drive the structuring of range-limited fossorial species. With ongoing environmental changes, it is crucial to utilize this knowledge to safeguard mountain biodiversity and ecosystem functioning.

Acknowledgements

This work was supported by the German Research Council (DFG) in the framework of the joint Ethio-European DFG Research Unit 2358 "The Mountain Exile Hypothesis. How humans benefited from and re-shaped African high-altitude ecosystems during Quaternary climate changes" [FA-925/14-1], [OP-219/10-2] and [SCHA-2085/3-1]. We are grateful to the Ethiopian Wildlife Conservation Authority, the College of Natural and Computational Sciences (Addis Ababa University), the Department of Plant

Biology and Biodiversity Management (Addis Ababa University), the Frankfurt Zoological Society, the Ethiopian Wolf Project, and the Bale Mountains National Park for their cooperation and kind permission to conduct fieldwork. We are thankful to Awol Assefa, Wege Abebe, Mohammed Ahmed Muhammed and Katinka Thielsen for contributing to the preparation and implementation of the fieldwork, Christian Lampei for input on landscape genetic analyses, Alexander Groos for the input on Late Pleistocene glaciation, and Usman Abdella, Hamza Ahmed, Mohammed Kadir, Kasim Adem, Hussein Umer and Sophie Haje, for their great assistance in the field. The research was also supported by Villum Fonden Young Investigator Programme, grant no 13151 and Independent Research Fund Denmark, Sapere Aude: DFF-Forskningsleder, grant no 9064-00025B to EDL.

Data Accessibility

The mitochondrial genome data that support the findings of this study will be openly available in GenBank of NCBI at https://www.ncbi.nlm.nih.gov under accession no. OQ207545-OQ207620 and MW751806, upon acceptance of this paper. The raw sequencing reads will be available in the associated BioProject PRJNA940645.

Author contributions

NF, GM, LO, TW and DGS designed the research concept and NF, LO and DGS secured the project funding. VMR, AA, LW and DGS captured specimens in the field. VMR and AR-I conducted lab work. VMR, AR-I and MVW analysed the data with contributions from RS, EDL, and DGS for genetic and ecological interpretation. LW generated raster layers for landscape genetic analyses. VMR, EDL and DGS wrote the manuscript with contributions from all co-authors. All authors gave final approval for publication and agreed to be held accountable for the work carried out within this publication.

References

Akaike, H. (1974). A New Look at the Statistical Model Identification. *IEEE Transactions on Automatic Control*, *19*(6), 716–723.

Alexander, A. (2017). *genetic_diversity_diffs v1.0.3*. https://github.com/laninsky/genetic_diversity_diffs

Asefa, A., Reuber, V., Miehe, G., Wondafrash, M., Wraase, L., Wube, T., Farwig, N., & Schabo, D. G. (2022). The activity of a subterranean small mammal alters Afroalpine vegetation patterns and is positively affected by livestock grazing. *Basic and Applied Ecology*.

Avise, J. C. (2000). *Phylogeography: the history and formation of species*. Havard University Press.

Badgley, C., Smiley, T. M., Terry, R., Davis, E. B., DeSantis, L. R. G., Fox, D. L., Hopkins, S. S. B., Jezkova, T., Matocq, M. D., Matzke, N., McGuire, J. L., Mulch, A., Riddle, B. R., Roth, V. L., Samuels, J. X., Strömberg, C. A. E., & Yanites, B. J. (2017). Biodiversity and Topographic Complexity: Modern and Geohistorical Perspectives. *Trends in Ecology and Evolution*, *32*(3), 211–226.

Begall, S., Burda, H., & Schleich, C. E. (2007). *Subterranean rodents : news from underground*. Springer.

Berthier, K., Galan, M., Foltête, J. C., Charbonnel, N., & Cosson, J. F. (2005). Genetic structure of the cyclic fossorial water vole (Arvicola terrestris): Landscape and demographic influences. *Molecular Ecology*, *14*(9), 2861–2871.

Birky, W. C., Maruyama, T., & Fuerst, P. (1983). An approach to population and evolutionary genetic theory for genes in mitochondria and chloroplasts, and some results. *Genetics*, *103*, 513–527.

Boulangeat, I., Gravel, D., & Thuiller, W. (2012). Accounting for dispersal and biotic interactions to disentangle the drivers of species distributions and their abundances. *Ecology Letters*, *15*(6), 584–593.

Brown, J. H. (2001). Mammals on mountainsides: elevational patterns of diversity. *Global Ecology and Biogeography*, *10*(1), 101–109.

Bryja, J., Granjon, L., Dobigny, G., Patzenhauerová, H., Konečný, A., Duplantier, J. M., Gauthier, P.,

Colyn, M., Durnez, L., Lalis, A., & Nicolas, V. (2010). Plio-Pleistocene history of West African Sudanian savanna and the phylogeography of the Praomys daltoni complex (Rodentia): The environment/geography/genetic interplay. *Molecular Ecology*, *19*(21), 4783–4799.

Carøe, C., Gopalakrishnan, S., Vinner, L., Mak, S. S. T., Sinding, M. H. S., Samaniego, J. A., Wales, N., Sicheritz-Pontén, T., & Gilbert, M. T. P. (2018). Single-tube library preparation for degraded DNA. *Methods in Ecology and Evolution*, *9*(2), 410–419.

Chu, B., Ji, C., Zhou, J., Zhou, Y., & Hua, L. (2021). Why does the plateau zokor (Myospalax fontanieri: Rodentia: Spalacidae) move on the ground in summer in the eastern Qilian Mountains? *Journal of Mammalogy*, *102*(1), 346–357.

Clarke, R. T., Rothery, P., & Raybould, A. F. (2002). Confidence limits for regression relationships between distance matrices: Estimating gene flow with distance. *Journal of Agricultural, Biological, and Environmental Statistics*, *7*(3), 361–372.

Cunningham, H. R., Rissler, L. J., Buckley, L. B., & Urban, M. C. (2016). Abiotic and biotic constraints across reptile and amphibian ranges. *Ecography*, *39*(1), 1–8.

Cushman, S. A., & Landguth, E. L. (2010). Spurious correlations and inference in landscape genetics. *Molecular Ecology*, *19*(17), 3592–3602.

Cushman, S. A., & Lewis, J. S. (2010). Movement behavior explains genetic differentiation in American black bears. *Landscape Ecology*, *25*(10), 1613–1625.

Cushman, S. A., McKelvey, K. S., Hayden, J., & Schwartz, M. K. (2006). Gene flow in complex landscapes: Testing multiple hypotheses with causal modeling. *American Naturalist*, *168*(4), 486–499.

Cutrera, A. P., Lacey, E. A., & Busch, C. (2005). Genetic structure in a solitary rodent (Ctenomys talarum): Implications for kinship and dispersal. *Molecular Ecology*, *14*(8), 2511–2523.

Davies, T. J., Purvis, A., & Gittleman, J. L. (2009). Quaternary climate change and the geographic ranges of mammals. *American Naturalist*, *174*(3), 297–307.

Excoffier, L., & Lischer, H. E. L. (2010). Arlequin suite ver 3.5: A new series of programs to perform

population genetics analyses under Linux and Windows. *Molecular Ecology Resources*, *10*(3), 564–567.

Fernández-Stolz, G. P., Stolz, J. F. B., & De Freitas, T. R. O. (2007). Bottlenecks and dispersal in the tuco-tuco das dunas, Ctenomys flamarioni (Rodentia: Ctenomyidae), in Southern Brazil. *Journal of Mammalogy*, *88*(4), 935–945.

Finn, K. T., Thorley, J., Bensch, H. M., & Zöttl, M. (2022). Subterranean Life-Style Does Not Limit Long Distance Dispersal in African Mole-Rats. *Frontiers in Ecology and Evolution*, *10*.

Gashaw, T. (2015). Threats of Bale Mountains National Park and solutions, Ethiopia. *Journal of Physical Science and Environmental Studies*, *1*(2), 10–16.

Gaston, K. J. (2003). *The stucture and dynamics of geographic ranges*. Oxford University Press.

Groos, A. R., Akçar, N., Yesilyurt, S., Miehe, G., Vockenhuber, C., & Veit, H. (2021). Nonuniform late pleistocene glacier fluctuations in tropical Eastern Africa. *Science Advances*, *7*(11).

Guo, Y. T., Zhang, J., Xu, D. M., Tang, L. Z., & Liu, Z. (2021). Phylogenomic relationships and molecular convergences to subterranean life in rodent family Spalacidae. *Zoological Research*, *42*(5), 671–674.

Harestad, A. S., & Bunnel, F. L. (1979). Home Range and Body Weight--A Reevaluation. *Ecology*, *60*(2), 389–402.

Hewitt, G. M. (1996). Some genetic consequences of ice ages, and their role in divergence and speciation. *Biological Journal of the Linnean Society*, *58*(3), 247–276.

Hewitt, G. M. (2004). The structure of biodiversity - Insights from molecular phylogeography. *Frontiers in Zoology*, *1*, 1–16.

Hoffmann, A. A., Sgrò, C. M., & Kristensen, T. N. (2017). Revisiting Adaptive Potential, Population Size, and Conservation. *Trends in Ecology and Evolution*, *32*(7), 506–517.

Kawalika, M., & Burda, H. (2007). Giant Mole-rats, Fukomys mechowii, 13 Years on the Stage. In S. Begall, H. Burda, & C. E. Schleich (Eds.), *Subterranean Rodents: News from Underground* (pp. 205–

219). Springer.

Korneliussen, T. S., Albrechtsen, A., & Nielsen, R. (2014). ANGSD: Analysis of Next Generation Sequencing Data. *BMC Bioinformatics*, *15*(1), 1–13.

Lande, R. (1988). Genetics and demography in biological conservation. *Science*, *241*(4872), 1455–1460.

Lanfear, R., Frandsen, P. B., Wright, A. M., Senfeld, T., & Calcott, B. (2017). Partitionfinder 2: New methods for selecting partitioned models of evolution for molecular and morphological phylogenetic analyses. *Molecular Biology and Evolution*, *34*(3), 772–773.

Lavrenchenko, L., & Kennerley, R. (2016). *Tachyoryctes macrocephalus, The IUCN Red List of Threatened Species 2016: e.T21293A115161321*.

Le Galliard, J. F., Rémy, A., Ims, R. A., & Lambin, X. (2012). Patterns and processes of dispersal behaviour in arvicoline rodents. *Molecular Ecology*, *21*(3), 505–523.

Leigh, J. W., & Bryant, D. (2015). POPART: Full-feature software for haplotype network construction. *Methods in Ecology and Evolution*, *6*(9), 1110–1116.

Li, H., & Durbin, R. (2009). Fast and accurate short read alignment with Burrows–Wheeler transform. *Bioinformatics*, *25*(14), 1754–1760.

Li, H., Handsaker, B., Wysoker, A., Fennell, T., Ruan, J., Homer, N., Marth, G., Abecasis, G., & Durbin, R. (2009). The Sequence Alignment/Map format and SAMtools. *Bioinformatics*, *25*(16), 2078–2079.

Magoč, T., & Salzberg, S. L. (2011). FLASH: Fast length adjustment of short reads to improve genome assemblies. *Bioinformatics*, *27*(21), 2957–2963.

Manel, S., Gugerli, F., Thuiller, W., Alvarez, N., Legendre, P., Holderegger, R., Gielly, L., & Taberlet, P. (2012). Broad-scale adaptive genetic variation in alpine plants is driven by temperature and precipitation. *Molecular Ecology*, *21*(15), 3729–3738.

Mapelli, F. J., Mora, M. S., Mirol, P. M., & Kittlein, M. J. (2012). Population structure and landscape genetics in the endangered subterranean rodent Ctenomys porteousi. *Conservation Genetics*, *13*(1), 165–181.

Meisner, J., & Albrechtsen, A. (2018). Inferring Population Structure and Admixture Proportions in Low-Depth NGS Data. *Genetics*, *210*(2), 719–731.

Mekonen, S. (2020). Coexistence between human and wildlife: The nature, causes and mitigations of human wildlife conflict around Bale Mountains National Park, Southeast Ethiopia. *BMC Ecology*, *20*(1), 1–9.

Miehe, S., & Miehe, G. (1994). Ericaceous forests and heathlands in the Bale Mountains of South Ethiopia. In *Ecology and Man's Impact*. Traute Warnke, Hamburg.

Mirol, P., Giménez, M. D., Searle, J. B., Bidau, C. J., & Faulkes, C. G. (2010). Population and species boundaries in the South American subterranean rodent Ctenomys in a dynamic environment. *Biological Journal of the Linnean Society*, *100*(2), 368–383.

Mora, M. S., Mapelli, F. J., Gaggiotti, O. E., Kittlein, M. J., & Lessa, E. P. (2010). Dispersal and population structure at different spatial scales in the subterranean rodent Ctenomys australis. *BMC Genetics*, *11*(9).

Nevo, E. (1999). *Mosaic evolution of subterranean mammals: regression, progression and global convergence*. Oxford Univ Press.

Oksanen, J., Legendre, P., O'Hara, B., Stevens, M. H. H., Oksanen, M. J., & Suggests, M. (2020). Vegan: Community Ecology Package. R package version 2.5-7. In *Community ecology package* (Vol. 10, pp. 631–637).

Ossendorf, G., Groos, A. R., Bromm, T., Tekelemariam, M. G., Glaser, B., Lesur, J., Schmidt, J., Akçar, N., Bekele, T., Beldados, A., Demissew, S., Kahsay, T. H., Nash, B. P., Nauss, T., Negash, A., Nemomissa, S., Veit, H., Vogelsang, R., Woldu, Z., … Miehe, G. (2019). Middle Stone Age foragers resided in high elevations of the glaciated Bale Mountains, Ethiopia. *Science*, *365*(6453), 583–587.

Parmesan, C. (2006). Ecological and evolutionary responses to recent climate change. In *Annual Review of Ecology, Evolution, and Systematics* (Vol. 37, pp. 637–669). Annual Reviews.

Peterman, W. E. (2018). ResistanceGA: An R package for the optimization of resistance surfaces using genetic algorithms. *Methods in Ecology and Evolution*, *9*(6), 1638–1647.

Peterman, W. E., Connette, G. M., Semlitsch, R. D., & Eggert, L. S. (2014). Ecological resistance surfaces predict fine-scale genetic differentiation in a terrestrial woodland salamander. *Molecular Ecology*, *23*(10), 2402–2413.

Quaglietta, L., Fonseca, V. C., Hájková, P., Mira, A., & Boitani, L. (2013). Fine-scale population genetic structure and short-range sex-biased dispersal in a solitary carnivore, Lutra lutra. *Journal of Mammalogy*, *94*(3), 561–571.

R Core Team. (2021). *R: A Language and Environment for Statistical Computing. R Foundation for Statistical Computing*. https://www.r-project.org/

Rahbek, C., Borregaard, M. K., Antonelli, A., Colwell, R. K., Holt, B. G., Nogues-Bravo, D., Rasmussen, C. M. Ø., Richardson, K., Rosing, M. T., Whittaker, R. J., & Fjeldså, J. (2019). Building mountain biodiversity: Geological and evolutionary processes. *Science*, *365*(6458), 1114–1119.

Rahbek, C., Borregaard, M. K., Colwell, R. K., Dalsgaard, B., Holt, B. G., Morueta-Holme, N., Nogues-Bravo, D., Whittaker, R. J., & Fjeldså, J. (2019). Humboldt's enigma: What causes global patterns of mountain biodiversity? *Science*, *365*(6458), 1108–1113.

Reichman, O. J. (1975). Relation of Desert Rodent Diets to Available Resources. *Journal of Mammalogy*, *56*(4), 731–751. https://doi.org/10.2307/1379649

Reuber, V. M., Rey-Iglesia, A., Westbury, M. V., Cabrera, A. A., Farwig, N., Skovrind, M., Šumbera, R., Wube, T., Opgenoorth, L., Schabo, D. G., & Lorenzen, E. D. (2021). Complete mitochondrial genome of the giant root-rat (Tachyoryctes macrocephalus). *Mitochondrial DNA Part B: Resources*, *6*(8), 2191–2193.

Rice, W. R. (1989). Analyzing tables of statistical tests. *Evolution*, *43*, 223–225.

Ronquist, F., & Huelsenbeck, J. P. (2003). MrBayes 3: Bayesian phylogenetic inference under mixed models. *Bioinformatics*, *19*(12), 1572–1574.

Rousset, F. (1997). Genetic differentiation and estimation of gene flow from F-statistics under isolation by distance. *Genetics*, *145*(4), 1219–1228.

Rozas, J., Sánchez-DelBarrio, J. C., Messeguer, X., & Rozas, R. (2003). DnaSP, DNA polymorphism analyses by the coalescent and other methods. *Bioinformatics*, *19*(18), 2496–2497.

Ruiz-Gonzalez, A., Cushman, S. A., Madeira, M. J., Randi, E., & Gómez-Moliner, B. J. (2015). Isolation by distance, resistance and/or clusters? Lessons learned from a forest-dwelling carnivore inhabiting a heterogeneous landscape. *Molecular Ecology*, *24*(20), 5110–5129.

Sandel, B., Arge, L., Dalsgaard, B., Davies, R. G., Gaston, K. J., Sutherland, W. J., & Svenning, J. C. (2011). The influence of late quaternary climate-change velocity on species endemism. *Science*, *334*(6056), 660–664.

Schweizer, M., Excoffier, L., & Heckel, G. (2007). Fine-scale genetic structure and dispersal in the common vole (Microtus arvalis). *Molecular Ecology*, *16*(12), 2463–2473.

Scrucca, L. (2013). GA: A Package for Genetic Algorithms in R. *Journal of Statistical Software*, *53*(4), 1–37.

Sexton, J. P., McIntyre, P. J., Angert, A. L., & Rice, K. J. (2009). Evolution and ecology of species range limits. *Annual Review of Ecology, Evolution, and Systematics*, *40*, 415–436.

Shirk, A. J., Landguth, E. L., & Cushman, S. A. (2018). A comparison of regression methods for model selection in individual-based landscape genetic analysis. *Molecular Ecology Resources*, *18*(1), 55–67.

Sillero-Zubiri, C., & Gottelli, D. (1995). Diet and Feeding Behavior of Ethiopian Wolves (Canis simensis). *Journal of Mammalogy*, *76*(2), 531–541.

Sillero-Zubiri, C., Tattersall, F. H., & Macdonald, D. W. (1995). Habitat selection and daily activity of giant molerats Tachyoryctes macrocephalus: Significance to the Ethiopian wolf Canis simensis in the Afroalpine ecosystem. *Biological Conservation*, *72*(1), 77–84.

Šklíba, J., Vlasatá, T., Lövy, M., Hrouzková, E., Meheretu, Y., Sillero-Zubiri, C., & Šumbera, R. (2017).

Ecological role of the giant root-rat (Tachyoryctes macrocephalus) in the Afroalpine ecosystem. *Integrative Zoology*, *12*(4), 333–344.

Šklíba, J., Vlasatá, T., Lövy, M., Hrouzková, E., Meheretu, Y., Sillero-Zubiri, C., & Šumbera, R. (2020). The giant that makes do with little: small and easy-to-leave home ranges found in the giant root-rat. *Journal of Zoology*, *310*(1), 64–70.

Skotte, L., Korneliussen, T. S., & Albrechtsen, A. (2013). Estimating individual admixture proportions from next generation sequencing data. *Genetics*, *195*(3), 693–702.

Stephens, P. A., D'Sa, C. A., Sillero-Zubiri, C., & Leader-Williams, N. (2001). Impact of livestock and settlement on the large mammalian wildlife of Bale Mountains National Park, southern Ethiopia. *Biological Conservation*, *100*(3), 307–322.

Šumbera, R., Lövy, M., Marino, J., Šimek, M., & Šklíba, J. (2020). Gas composition and its daily changes within burrows and nests of an Afroalpine fossorial rodent, the giant root-rat Tachyoryctes macrocephalus. *Zoology*, *142*, 125819.

Tallents, L. A., & Macdonald, D. W. (2011). Mapping High-Altitude Vegetation in the Bale Mountains, Ethiopia. *Walia—Special Edition on the Bale Mountains*, 97–117.

Tromp-van Meerveld, H. J., & McDonnell, J. J. (2006). On the interrelations between topography, soil depth, soil moisture, transpiration rates and species distribution at the hillslope scale. *Advances in Water Resources*, *29*(2), 293–310.

Tucker, M. A., Ord, T. J., & Rogers, T. L. (2014). Evolutionary predictors of mammalian home range size: Body mass, diet and the environment. *Global Ecology and Biogeography*, *23*(10), 1105–1114.

Vlasatá, T., Šklíba, J., Lövy, M., Meheretu, Y., Sillero-Zubiri, C., & Šumbera, R. (2017). Daily activity patterns in the giant root rat (Tachyoryctes macrocephalus), a fossorial rodent from the Afro-alpine zone of the Bale Mountains, Ethiopia. *Journal of Zoology*, *302*(3), 157–163.

Weir, B. S., & Cockerham, C. C. (1984). *Estimating F-Statistics for the Analysis of Population Structure*. *38*(6), 1358–1370.

Westbury, M. V., Hartmann, S., Barlow, A., Wiesel, I., Leo, V., Welch, R., Parker, D. M., Sicks, F., Ludwig, A., Dalen, L., & Hofreiter, M. (2018). Extended and Continuous Decline in Effective Population Size Results in Low Genomic Diversity in the World's Rarest Hyena Species, the Brown Hyena. *Molecular Biology and Evolution*, *35*(5), 1225–1237.

Willi, Y., Van Buskirk, J., & Hoffmann, A. A. (2006). Limits to the adaptive potential of small populations. *Annual Review of Ecology, Evolution, and Systematics*, *37*, 433–458.

Wilson, R. J., & Gutiérres, D. (2016). Effects of Climate Change on the Elevational Limits of Species Ranges. In *Ecological Consequences of Climate Change: Mechanisms, Conservation, and Management* (pp. 107–132).

Wraase, L., Reuber, V. M., Kurth, P., Fekadu, M., Demissew, S., Miehe, G., Opgenoorth, L., Selig, U., Woldu, Z., Zeuss, D., Schabo, D. G., Farwig, N., & Nauss, T. (2022). Remote sensing-supported mapping of the activity of a subterranean landscape engineer across an afro-alpine ecosystem. *Remote Sensing in Ecology and Conservation*, 1–15.

Wright, S. (1969). *Evolution and the genetics of populations, vol. 2, The Theory of Gene Frequencies*. University of Chicago Press.

Wright, S. (1978). *Evolution and the genetics of populations, vol. 4: variability within and among natural populations*. University of Chicago Press.

Yaba, M., Mekonnen, T., Bekele, A., & Malcolm, J. (2011). Food selection and feeding behavior of giant mole rat (Tachyoryctes macrocephalus, Ruppell, 1842) from the sanetti plateau of bale mountains national park, Ethiopia. In *Asian Journal of Applied Sciences* (Vol. 4, Issue 7, pp. 735–740).

Yalden, D. W. (1985). Tachyoryctes macrocephalus. *Mammalian Species*, *237*, 1–3.

Yalden, D. W., & Largen, M. J. (1992). The endemic mammals of Ethiopia. *Mammal Review*, *22*(3–4), 115–150.

Zagorodniuk, I., Korobchenko, M., Parkhomenko, V., & Barkaszi, Z. (2018). Steppe rodents at the edge

of their range: A case study of Spalax microphthalmus in the north of Ukraine. *Biosystems Diversity*, *26*(3), 188–200.

Zhang, Y. (2007). The Biology and Ecology of Plateau Zokors (Eospalax fontanierii). In S. Begall, H. Burda, & C. E. Schleich (Eds.), *Subterranean Rodents: News from Underground* (pp. 237–249). Springer.